Science Bulletin 67 (2022) 479–487

Contents lists available at ScienceDirect

Science Bulletin

journal homepage: www.elsevier.com/locate/scib

Science Bulletin
www.scibull.com

Article

Measurement of the lifetimes of promptly produced Ω_c^0 and Ξ_c^0 baryons

LHCb Collaboration [1]

ARTICLE INFO

Article history:
Received 6 September 2021
Received in revised form 28 October 2021
Accepted 17 November 2021
Available online 1 December 2021

Keywords:
Charmed baryon
Flavour physics
QCD
Lifetime
Charm physics
LHCb

ABSTRACT

A measurement of the lifetimes of the Ω_c^0 and Ξ_c^0 baryons is reported using proton–proton collision data at a centre-of-mass energy of 13 TeV, corresponding to an integrated luminosity of 5.4 fb^{-1} collected by the LHCb experiment. The Ω_c^0 and Ξ_c^0 baryons are produced directly from proton interactions and reconstructed in the $pK^-K^-\pi^+$ final state. The Ω_c^0 lifetime is measured to be $276.5 \pm 13.4 \pm 4.4 \pm 0.7$ fs, and the Ξ_c^0 lifetime is measured to be $148.0 \pm 2.3 \pm 2.2 \pm 0.2$ fs, where the first uncertainty is statistical, the second systematic, and the third due to the uncertainty on the D^0 lifetime. These results confirm previous LHCb measurements based on semileptonic beauty-hadron decays, which disagree with earlier results of a four times shorter Ω_c^0 lifetime, and provide the single most precise measurement of the Ω_c^0 lifetime.
© 2021 Science China Press. Published by Elsevier B.V. and Science China Press. This is an open access article under the CC BY license (http://creativecommons.org/licenses/by/4.0/).

1. Introduction

The LHCb Collaboration has previously measured the lifetimes of Ω_c^0 and Ξ_c^0 baryons, with valence quark content of *ssc* and *dsc*, respectively, using candidates from semileptonic beauty-hadron decays [1,2]. The measured Ω_c^0 lifetime, $\tau_{\Omega_c^0}$, is nearly four times larger than the previous world average [3], which is inconsistent at a level of seven standard deviations. The measured Ξ_c^0 lifetime, $\tau_{\Xi_c^0}$, is larger than the previous world average by three standard deviations. Resolving these discrepancies is important for theoretical calculations. Lifetime measurements of hadrons containing heavy quarks Q, i.e., charm or beauty quarks, provide input needed to test precisely the Standard Model and search for physics beyond.

Heavy quark expansion [4–11] is an effective theory used to calculate the lifetimes of these hadrons through an expansion in inverse powers of the mass of the heavy quark, m_Q. The lowest-order term in the expansion depends only on m_Q and contributes equally to the decay width of all hadrons with the same heavy quark. Differences in predicted lifetimes are expected to arise from higher-order effects, such as weak W-annihilation and Pauli interference, due to the presence of different spectator quarks. Measurements of charmed-hadron lifetimes are particularly sensitive to these higher-order contributions, as these corrections typically increase as m_Q decreases and are large for charmed hadrons [12–17]. A lifetime hierarchy of $\tau_{\Xi_c^+} > \tau_{\Lambda_c^+} > \tau_{\Xi_c^0} > \tau_{\Omega_c^0}$ is obtained considering higher-order effects [13,15–18], whereas the ordering of $\tau_{\Xi_c^+} > \tau_{\Omega_c^0} > \tau_{\Lambda_c^+} > \tau_{\Xi_c^0}$ can be obtained depending on the treatment of even higher-order effects [17,19,20]. Knowledge on the lifetimes is also required to make comparisons between measured branching fractions of charmed baryons and corresponding theoretical predictions for their partial decay widths.

The LHCb experiment has recorded an unprecedented number of charmed baryons, produced both at the primary proton–proton (pp) collision vertex (PV), referred to as prompt, and from decays of beauty hadrons. In this paper, a measurement of the lifetimes of Ω_c^0 and Ξ_c^0 baryons is reported based on a sample of Ω_c^0 and Ξ_c^0 baryons promptly produced in pp collisions at a centre-of-mass energy of 13 TeV. The data sample was collected by the LHCb experiment between 2016–2018 and corresponds to an integrated luminosity of 5.4 fb^{-1}. The Ω_c^0 and Ξ_c^0 baryons are reconstructed in the $pK^-K^-\pi^+$ final state.[2] In order to avoid experimenter's bias, the results of the analysis were not examined until the full procedure had been finalised. Prompt $D^0 \to K^+K^-\pi^+\pi^-$ decays are used as a control mode in order to reduce systematic uncertainties and to validate the analysis procedure.

2. Detector and simulation

The LHCb detector [21,22] is a single-arm forward spectrometer covering the pseudorapidity range $2 < \eta < 5$, designed for the

[1] Authors are listed at the end of this paper.

[2] The inclusion of charge-conjugate processes is implied throughout.

https://doi.org/10.1016/j.scib.2021.11.022
2095-9273/© 2021 Science China Press. Published by Elsevier B.V. and Science China Press.
This is an open access article under the CC BY license (http://creativecommons.org/licenses/by/4.0/).

study of particles containing b or c quarks. The tracking system provides a measurement of the momentum, p, of charged particles with a relative uncertainty that varies from 0.5% at low momentum to 1.0% at 200 GeV/c. The minimum distance of a track to a PV, the impact parameter (IP), is measured with a resolution of $(15 + 29/p_{\mathrm{T}})$ μm, where p_{T} is the component of the momentum transverse to the beam, in GeV/c. Different types of charged hadrons are distinguished using information from two ring-imaging Cherenkov detectors. Photons, electrons and hadrons are identified by a calorimeter system consisting of scintillating-pad and preshower detectors, an electromagnetic and a hadronic calorimeter. The online event selection is performed by a trigger, which consists of a hardware stage, based on information from the calorimeter and muon systems, followed by a two-level software stage, which applies a full event reconstruction. Between the two software stages, an alignment and calibration of the detector is performed in near real-time and their results are used in the trigger. The same alignment and calibration information is propagated to the offline reconstruction, ensuring consistent and high-quality particle identification (PID) information between the trigger and offline software. The identical performance of the online and offline reconstruction offers the opportunity to perform physics analyses directly using candidates reconstructed in the trigger [23,24], which this analysis utilises.

Simulated samples are used to model the effects of the detector acceptance and the imposed selection requirements, and to study the modelling of the discriminating variables between signal and background candidates. In the simulation, pp collisions are generated using PYTHIA [25,26] with a specific LHCb configuration [27]. Decays of unstable particles are described by EVTGEN [28], in which final-state radiation is generated using PHOTOS [29]. The interaction of the generated particles with the detector, and its response, are implemented using the GEANT4 toolkit [30,31] as described in Ref. [32]. The underlying pp interaction is reused multiple times, with an independently generated signal decay for each [33].

3. Candidate selection

Candidate decays of charmed hadrons are reconstructed through the $\Omega_c^0 \to pK^-K^-\pi^+$, $\Xi_c^0 \to pK^-K^-\pi^+$, and $D^0 \to K^+K^-\pi^+\pi^-$ decay modes. All final-state charged particle candidates are required to be inconsistent with originating from any PV. The PV associated to a single charged particle is defined to be the PV with the smallest χ^2_{IP}, where χ^2_{IP} is defined as the difference in the vertex-fit χ^2 of a given PV reconstructed with and without the given particle. Each of the final-state particles is required to have good track quality, large transverse and total momentum, and particle-identification information consistent with the corresponding p, K, or π hypothesis. The angle between each pair of final-state particles is required to be larger than 0.5 mrad to avoid selecting duplicate tracks. The charmed hadron candidates are required to have a decay vertex with good quality that is displaced from its associated PV. The angle between the reconstructed momentum vector of a charmed baryon candidate and the direction from its associated PV to its decay vertex, the direction angle, is required to be small to suppress combinatorial background.

To improve further the signal purity, a multivariate classifier is trained based on the adaptive boosted decision tree (BDT) algorithm [34,35] implemented in the TMVA toolkit [36,37]. The classifier is trained using simulated prompt $\Omega_c^0 \to pK^-K^-\pi^+$ decays as signal, and data from the Ω_c^0 mass sidebands of $25 < |m(pK^-K^-\pi^+) - m_{\Omega_c^0}| < 75\ \mathrm{MeV}/c^2$ as background. Here, $m(pK^-K^-\pi^+)$ is the invariant mass of the decay products of the charmed baryon candidate and $m_{\Omega_c^0}$ is the known Ω_c^0 mass [38]. The sideband ranges from 5 to 14 times the invariant-mass resolution. The lifetime of the simulated Ω_c^0 decays is 250 fs. Eleven input variables are used in the training, including: the χ^2 of the Ω_c^0 decay-vertex fit; the transverse momentum, pseudorapidity and the direction angle of the Ω_c^0 candidate; the transverse momenta as well as the minimal transverse momentum of the four final-state particles; and the natural logarithm of the sum and minimum χ^2_{IP} of the four final-state particles. A requirement on the BDT response is chosen which selects approximately 99% of Ω_c^0 signal decays while rejecting about 60% of the background. The same requirement is also applied to the Ξ_c^0 signal decays. The number of signal candidates for the Ω_c^0, Ξ_c^0, and D^0 decay modes are determined using the $[2645, 2745]$, $[2421, 2521]$, and $[1835, 1915]\ \mathrm{MeV}/c^2$ invariant-mass regions, respectively.

Specific trigger requirements are applied to candidates to ensure a precise estimation of the selection efficiency as a function of decay time. In the offline selection, trigger signals are associated with reconstructed particles. Selection requirements can therefore be made on the trigger selection itself and if the decision was due to the signal candidate. At the hardware stage, at least one of the final-state tracks is required to deposit large transverse energy in the hadronic calorimeter. At the software stage, at least one of the final-state tracks is required to pass a MatrixNet classifier [39], which is trained to select displaced tracks [40].

4. Prompt yield determination

Charmed hadron candidates are split into intervals of their decay time, which is calculated using the PV, its decay vertex, and its measured momentum. The signal yields are then determined in each interval. The interval boundaries of the Ω_c^0 sample are chosen to have a similar yield of Ω_c^0 signals in each interval, and correspond to $[0.45, 0.52, 0.57, 0.63, 0.69, 0.75, 0.81, 0.90, 1.05, 2.00]$ ps. For the Ξ_c^0 sample, the same boundaries are used except the last interval, which, for computational simplicity, is not included as the yield is consistent with zero. The same boundaries are used for the D^0 control mode as for the signal modes. Two variables are used to discriminate signal decays from different background contributions. One is the invariant mass of the charmed hadron, which is used to distinguish decays from combinatorial background due to the random combinations of tracks. The other is the logarithm of the χ^2_{IP} of the charmed hadron, $\log_{10}\chi^2_{\mathrm{IP}}$, which is used to separate prompt candidates from those produced in decays of beauty hadrons. The $\log_{10}\chi^2_{\mathrm{IP}}$ distribution for signal decays has smaller mean values than for those originating from beauty-hadron decays due to the lifetime of the ancestor beauty hadron.

Example distributions of invariant mass and $\log_{10}\chi^2_{\mathrm{IP}}$, in reduced mass regions around the peak, are presented in Fig. 1; the decay-time interval of $[0.69, 0.75]$ ps for data collected in 2018 is shown. To obtain the Ω_c^0, Ξ_c^0, and D^0 signal yields in each decay-time interval, two-dimensional unbinned extended maximum likelihood fits are performed to the invariant-mass and $\log_{10}\chi^2_{\mathrm{IP}}$ distributions. For each mode, the fits are performed simultaneously in all decay-time intervals and the three data-taking periods, 2016, 2017, and 2018. The invariant-mass distribution of the signal candidates is described with the sum of a Gaussian function and a double-sided Crystal Ball function [41] with a shared mean. The fit parameters are fixed to values obtained from simulation except for the mass peak and the effective resolution, which are obtained directly from data, but shared among the different decay-time intervals. The invariant-mass distribution of the combinatorial background contribution is described by a linear function with a slope left free

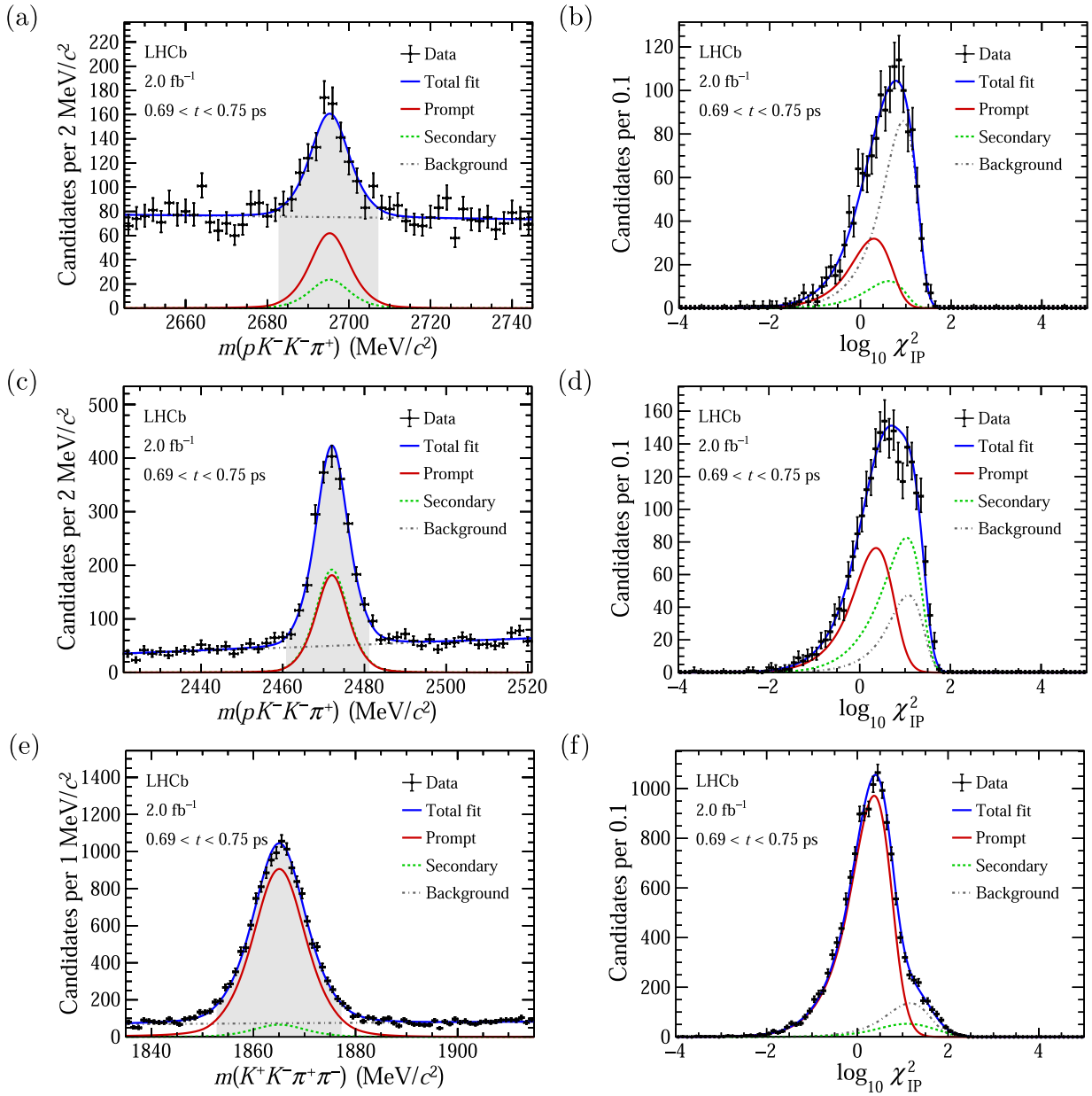


Fig. 1. (Color online) Distributions of (a) invariant mass and (b) $\log_{10}\chi^2_{\rm IP}$ in the reduced mass region of [2683, 2707] MeV/c^2 for the Ω_c^0 data sample, (c) invariant mass and (d) $\log_{10}\chi^2_{\rm IP}$ in the reduced mass region of [2461, 2481] MeV/c^2 for the Ξ_c^0 data sample, (e) invariant mass and (f) $\log_{10}\chi^2_{\rm IP}$ in the reduced mass region of [1853, 1877] MeV/c^2 for the D^0 data sample, along with the fit results. The sample is collected in 2018 in the decay-time interval of [0.69, 0.75] ps. The contributions of the signal, the secondary decays, and the combinatorial background are shown in red (solid), green (dashed), and gray (dash-dotted), respectively.

to vary in the fit. The $\log_{10}\chi^2_{\rm IP}$ distributions of both the signal and background components are described by a Bukin function [42]. For signal components, parameters of the Bukin function are fixed to values obtained from simulation except for the peak position that depends on the decay time. Here, an offset parameter is added to account for the disagreement between data and simulation. The offset parameter is free to vary and shared between decay-time intervals and data-taking periods in the fit. The parameters of the Bukin function of the combinatorial background contribution are fixed to values obtained from fits to the data samples in the side-band region as defined in the BDT training. The two-dimensional model used for signal, secondary decays, and background components is the product of the models for the invariant-mass and for the $\log_{10}\chi^2_{\rm IP}$ distributions. Fit projections to the invariant-mass and $\log_{10}\chi^2_{\rm IP}$ distribution are shown in Fig. 1.

5. Decay time fit

The lifetimes of the Ω_c^0 and Ξ_c^0 baryons are determined from a binned χ^2 fit comparing the signal yields in data with those from the simulation, where the lifetime is known. The latter is corrected using the control mode, as follows

$$\chi^2(\tau,\vec{C}) = \sum_j \sum_i \frac{\left(N^{\rm sig}_{i,j} - C_j \times F_i(\tau) \times R_{i,j}\right)^2}{\sigma^2_{N^{\rm sig}_{i,j}} + C_j^2 \times F_i^2(\tau) \times \sigma^2_{R_{i,j}}}, \qquad R_{i,j} = \frac{N^{\rm con}_{i,j}}{M^{\rm con}_{i,j}} \times M^{\rm sig}_{i,j}, \tag{1}$$

where $N^{\rm sig}_{i,j}$ ($N^{\rm con}_{i,j}$) is the signal yield in data for the signal (control) mode in decay-time interval i and for the data-taking period j, $M_{i,j}$ is the effective yield predicted from simulation, C_j is a normalisation

factor to account for the difference in size between the data and the simulated samples, and σ is the uncertainty of the relevant quantity. The difference in lifetime between data and simulated samples is accounted for by

$$F_i(\tau) = \frac{\int_i \exp(-t/\tau)\mathrm{d}t}{\int_i \exp(-t/\tau_{\rm sim})\mathrm{d}t} \times \frac{\int_i \exp(-t/\tau_{\rm sim}^{\rm con})\mathrm{d}t}{\int_i \exp(-t/\tau^{\rm con})\mathrm{d}t}, \quad (2)$$

where $\tau_{\rm sim} = 250$ fs is the signal mode lifetime in simulation and $\tau^{\rm con} = \tau_{\rm sim}^{\rm con}$ is the known D^0 lifetime [38], but is allowed to vary for estimating the systematic uncertainty. The resulting lifetime is $\tau_{\Omega_c^0} = 276.5 \pm 13.4$ fs with $\chi^2/\mathrm{ndf} = 22/23$ (ndf: number of degree of freedom) and $\tau_{\Xi_c^0} = 148.0 \pm 2.3$ fs with $\chi^2/\mathrm{ndf} = 30/20$, where the uncertainty is due to the limited size of the data and simulation samples. The result of the χ^2 fit to data is illustrated in Fig. 2, which shows the signal yield $N^{\rm sig}$ for selected candidates as a function of decay time, divided by the width of the corresponding decay-time interval, where the fit results are superimposed.

Several cross-checks are performed to ensure the robustness of the results. The χ^2 fit is performed to data of the $D^0 \to K^+K^-\pi^+\pi^-$ control mode for each data-taking period to validate the analysis procedure. The obtained lifetimes are consistent between data-taking periods and with the known D^0 lifetime [38]. The data samples are split into sub-samples according to data-taking periods and magnetic polarities of the LHCb dipole magnet, and the lifetimes are measured for each sub-sample. The resulting lifetimes are in good agreement with each other and with the default results. The measurement is repeated with two alternative boundaries of decay-time intervals and the obtained lifetimes are consistent with the default results within their statistical uncertainties. To ensure that the result is independent of the input lifetime used in simulation, the simulated signal decays are weighted to have alternative effective lifetimes within seven times the statistical uncertainty around the default lifetime. The χ^2 fit is then repeated. The difference of the obtained lifetimes with regard to the default fit is negligible.

6. Systematic uncertainties

Sources of systematic uncertainty are investigated and summarised in Table 1, including those due to the fit model, the limited size of the calibration samples, differences between data and simulation, and the uncertainty due to the choice of the D^0 control mode. The systematic uncertainty due to the modelling of $\log_{10}\chi^2_{\rm IP}$ is studied with the D^0 control mode. The following alternative models were tried and their impact on the signal yields studied. First, the effect due to fixed parameters in the Bukin function is studied by removing these constraints one at a time in the fit to the invariant-mass and $\log_{10}\chi^2_{\rm IP}$ distributions. Second, the uncertainty due to the choice of a single offset parameter for the peak positions of the Bukin functions across different decay-time intervals is studied by allowing independent offsets in each decay-time interval. Third, an alternative model for the $\log_{10}\chi^2_{\rm IP}$ distribution of the combinatorial background is obtained with the *sPlot* technique [43] using the invariant mass as the discriminating variable. Half of the largest difference between the signal yields from the alternative model fits is taken as the systematic uncertainty. The obtained systematic uncertainties on the signal yields are propagated to the measured lifetime using pseudoexperiments. In each pseudoexperiment, the yields of the signal and control modes are varied according to a Gaussian distribution whose mean is the value obtained with the default fit model and standard deviation the systematic uncertainty obtained with alternative models in the corresponding decay-time interval, and the lifetime is fit. The standard deviation of the distribution for the fitted lifetime is taken as the systematic uncertainty.

Table 1
Systematic uncertainties for the Ω_c^0 and Ξ_c^0 lifetimes.

Sources	$\tau_{\Omega_c^0}$ (fs)	$\tau_{\Xi_c^0}$ (fs)
Fit model	2.2	1.0
Calibration sample size	0.1	0.1
Kinematic correction	3.4	0.4
Decay-time resolution	1.3	1.8
$\chi^2_{\rm IP}$ scaling	1.1	0.5
Decay-length scale	0.1	0.1
D^0–$\bar{D}^0$ mixing	0.8	0.6
Total systematic uncertainty	4.4	2.2
D^0 lifetime	0.7	0.2
Statistical uncertainty	13.4	2.3

The selection efficiency of the hardware trigger is estimated in data using Λ_c^+ candidates from semileptonic Λ_b^0 decays [44]. The uncertainty due to the limited size of the calibration sample is estimated using pseudoexperiments, where the efficiency determined from the calibration sample is varied according to its uncertainty. The standard deviation of the distribution of the fitted lifetime is taken as the systematic uncertainty. The kinematic distributions of the simulated signal decays, including the transverse momentum and rapidity of the charmed hadron and the transverse momentum of final-state tracks, are weighted according to the dis-

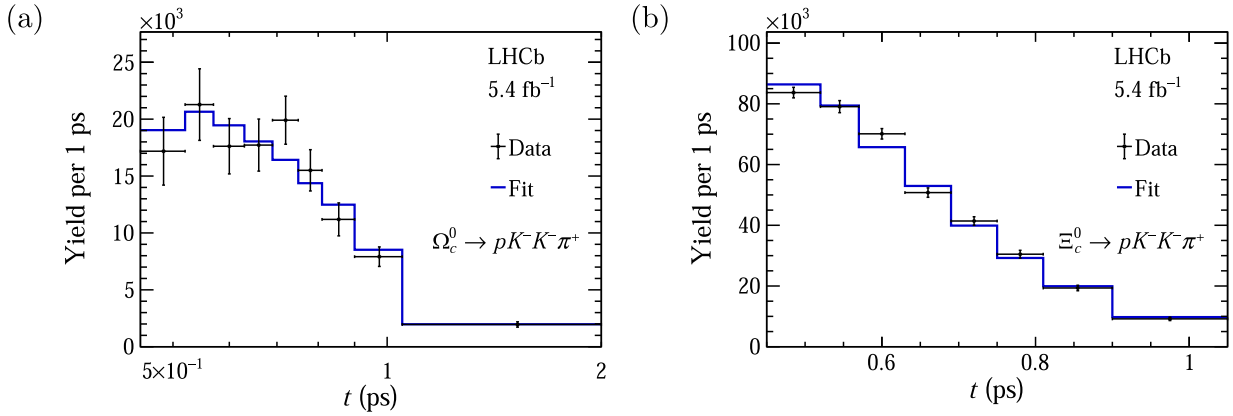


Fig. 2. (Color online) Decay-time distributions for the (a) Ω_c^0 mode and the (b) Ξ_c^0 mode with the χ^2 fit superimposed. The uncertainty on the data distribution is statistical only.

tributions observed in data for each mode. The impact of the limited size of the data samples, which is more pronounced for the Ω_c^0 mode, is studied with pseudoexperiments following the same procedure as described above.

Decay-time resolution in data is known to be different from simulation, although it cannot be accurately determined for the signal modes due to their limited yields in data. Nonetheless, the impact of this difference on the measured charm-hadron lifetimes largely cancels due to taking the ratio with the D^0 control mode. The residual effect is studied using pseudoexperiments and assigned as a systematic uncertainty. For these pseudoexperiments the D^0 control mode is generated with both a 30% larger and smaller decay-time resolution in the pseudo-data compared to pseudo-simulation, and the lifetime is fit. The difference between the input lifetime and the mean value of the distribution of the fitted lifetimes is taken as the systematic uncertainty.

The $\chi^2_{\rm IP}$ variables of the final-state tracks in simulation are scaled to account for differences between data and simulation for the data-taking periods of 2017 and 2018. The scaling factor is obtained by comparing data distributions in the control mode. The uncertainty on the scaling factor is determined to be 2%, based on χ^2 comparisons of data distributions with alternate scaling factors. The difference between the default fitted lifetime and the lifetime determined with a scaling factor varied by 2% is taken as the systematic uncertainty.

The measurement of the distance between the PV and the charmed-hadron decay vertex depends on the relative longitudinal positions of the vertex locator modules of the LHCb detector with respect to the beam axis. The uncertainty on the positions of the modules is estimated using survey measurements and the track based alignment [45,46], where the latter has the larger contribution. Its uncertainty does not cancel in the decay-time ratio and is taken as a relative systematic uncertainty of the measured lifetime.

The D^0 signal decays are reconstructed in a self-conjugate final state and D^0–$\bar{D}^0$ mixing is not considered in the χ^2 fit of the lifetime. The impact of D^0 mixing is estimated using pseudoexperiments in which the D^0 decay-time distribution is generated with mixing terms and the default χ^2 fit is performed to obtain the lifetime. The obtained difference between the input and resultant lifetime is assigned as a systematic uncertainty.

The known value of 410.1 fs [38] is assigned as D^0 lifetime in the default decay-time fit. The uncertainty on the D^0 lifetime, 1.5 fs [38], is propagated to the measured lifetime using pseudoexperiments. In each pseudoexperiment, the D^0 lifetime is varied according to its uncertainty. The standard deviation of the distribution for the fitted lifetime is taken as the systematic uncertainty.

7. Conclusion

In summary, a measurement of the lifetimes of the Ω_c^0 and Ξ_c^0 baryons is reported with Ω_c^0 and Ξ_c^0 baryons produced directly in proton–proton collisions at a centre-of-mass energy of 13 TeV, corresponding to an integrated luminosity of 5.4 fb^{-1} collected by the LHCb experiment. The Ω_c^0 lifetime is measured to be

$$\tau_{\Omega_c^0} = 276.5 \pm 13.4 \pm 4.4 \pm 0.7 \text{ fs}, \quad (3)$$

and the Ξ_c^0 lifetime is measured to be

$$\tau_{\Xi_c^0} = 148.0 \pm 2.3 \pm 2.2 \pm 0.2 \text{ fs}, \quad (4)$$

where the first uncertainty is statistical, the second systematic, and the third due to the uncertainty of the D^0 lifetime. This result is consistent with the previous LHCb measurements of the Ω_c^0 and Ξ_c^0 lifetimes, obtained from semileptonic beauty-hadron decays [1,2], and confirms the charmed-hadron lifetime hierarchy of $\tau_{\Xi_c^+} > \tau_{\Omega_c^0} > \tau_{\Lambda_c^+} > \tau_{\Xi_c^0}$. The precision of the Ω_c^0 lifetime is improved by a factor of two compared to that of the previous result [1].

This result is independent of previous LHCb measurements [1,2] due to the choice of independent data sample and analysis technique. Combining this measurement with previous LHCb measurements [1,2], given that both the statistical uncertainties and the dominant systematic uncertainties are uncorrelated, results in the weighted average lifetimes of

$$\begin{aligned} \tau_{\Omega_c^0} &= 274.5 \pm 12.4 \text{ fs}, \\ \tau_{\Xi_c^0} &= 152.0 \pm 2.0 \text{ fs}. \end{aligned} \quad (5)$$

The uncertainty includes both the statistical and systematic uncertainties.

Conflict of interest

The authors declare that they have no conflict of interest.

Acknowledgments

We express our gratitude to our colleagues in the CERN accelerator departments for the excellent performance of the LHC. We thank the technical and administrative staff at the LHCb institutes. We acknowledge support from CERN and from the national agencies: CAPES, CNPq, FAPERJ and FINEP (Brazil); MOST and NSFC (China); CNRS/IN2P3 (France); BMBF, DFG and MPG (Germany); INFN (Italy); NWO (Netherlands); MNiSW and NCN (Poland); MEN/IFA (Romania); MSHE (Russia); MICINN (Spain); SNSF and SER (Switzerland); NASU (Ukraine); STFC (United Kingdom); DOE NP and NSF (USA). We acknowledge the computing resources that are provided by CERN, IN2P3 (France), KIT and DESY (Germany), INFN (Italy), SURF (Netherlands), PIC (Spain), GridPP (United Kingdom), RRCKI and Yandex LLC (Russia), CSCS (Switzerland), IFIN-HH (Romania), CBPF (Brazil), PL-GRID (Poland) and OSC (USA). We are indebted to the communities behind the multiple open-source software packages on which we depend. Individual groups or members have received support from ARC and ARDC (Australia); AvH Foundation (Germany); EPLANET, Marie Skłodowska-Curie Actions and ERC (European Union); A*MIDEX, ANR, Labex P2IO and OCEVU, and Région Auvergne-Rhône-Alpes (France); Key Research Program of Frontier Sciences of CAS, CAS PIFI, CAS CCEPP, Fundamental Research Funds for the Central Universities, and Sci. & Tech. Program of Guangzhou (China); RFBR, RSF and Yandex LLC (Russia); GVA, XuntaGal and GENCAT (Spain); the Royal Society and the Leverhulme Trust (United Kingdom).

Appendix A. Supplementary materials

Supplementary materials to this article can be found online at https://doi.org/10.1016/j.scib.2021.11.022.

References

[1] LHCb Collaboration, Aaij R, et al. Measurement of the Ω_c^0 lifetime. Phys Rev Lett 2018;275:121.
[2] LHCb Collaboration, Aaij R, et al. Precision measurement of the Λ_c^+, Ξ_c^+, and Ξ_c^0 baryon lifetimes. Phys Rev D 2019;100:032001.
[3] Particle Data Group, Tanabashi M, et al. Review of particle physics. Phys Rev D 2018;98:030001.
[4] Khoze VA, Shifman MA. Heavy quarks. Sov Phys Usp 1983;26:387.
[5] Bigi IIY, Uraltsev NG. Gluonic enhancements in non-spectator beauty decays: an inclusive mirage though an exclusive possibility. Phys Lett B 1992;280:271.
[6] Bigi IIY, Uraltsev NG, Vainshtein AI. Nonperturbative corrections to inclusive beauty and charm decays: QCD versus phenomenological models. Phys Lett B 1992;293:430 (Erratum: Phys Lett B 1992;297:477).

[7] Blok B, Shifman MA. The rule of discarding $1/N_c$ in inclusive weak decays. (I). Nucl Phys B 1993;399:441.
[8] Blok B, Shifman MA. The rule of discarding $1/N_c$ in inclusive weak decays (II). Nucl Phys B 1993;399:459.
[9] Neubert M. *B* decays and the heavy quark expansion. Adv Ser Direct High Energy Phys 1998;15:239.
[10] Uraltsev N. Heavy quark expansion in beauty and its decays. Proc Int Sch Phys Fermi 1998;137:329.
[11] Bigi IIY. The QCD perspective on lifetimes of heavy flavor hadrons. arXiv: 9508408, 1995.
[12] Kirk M, Lenz A, Rauh T. Dimension-six matrix elements for meson mixing and lifetimes from sum rules. J High Energy Phys 2017;12:068 (Erratum: J High Energy Phys 2020;06:162).
[13] Cheng H-Y. Charmed baryons circa 2015. Front Phys 2015;10:101406.
[14] Lenz A, Rauh T. *D*-meson lifetimes within the heavy quark expansion. Phys Rev D 2013;88:034004.
[15] Bianco S, Fabbri FL, Benson D, et al. A cicerone for the physics of charm. Riv Nuovo Cim 2003;26:1.
[16] Bellini G, Bigi IIY, Dornan PJ. Lifetimes of charm and beauty hadrons. Phys Rep 1997;289:1.
[17] Blok B, Shifman MA. Lifetimes of charmed hadrons revisited. Facts and fancy. Talk at the Third Workshop on the Tau-Charm Factory: Marbella, Spain; 1993. arXiv: 9311331, 1993.
[18] Cheng H-Y. A Phenomenological analysis of heavy hadron lifetimes. Phys Rev D 1997;56:2783.
[19] Cheng H-Y. Phenomenological study of heavy hadron lifetimes. J High Energy Phys 2018;11:014.
[20] Cheng H-Y. Charmed baryon physics circa 2021. arXiv:2109.01216, 2021.
[21] LHCb Collaboration, Alves AA, et al. The LHCb detector at the LHC. J Instrum 2008;3:S08005.
[22] LHCb Collaboration, Aaij R, et al. LHCb detector performance. Int J Mod Phys A 2015;30:1530022.
[23] Aaij R, Albrecht J, Alessio F, et al. The LHCb trigger and its performance in 2011. J Instrum 2013;8:P04022.
[24] Aaij R, Amato S, Anderlini L, et al. Tesla: an application for real-time data analysis in high energy physics. Comput Phys Commun 2016;208:35.
[25] Sjöstrand T, Mrenna S, Skands P. PYTHIA 6.4 physics and manual. J High Energy Phys 2006;05:026.
[26] Sjöstrand T, Mrenna S, Skands P. A brief introduction to PYTHIA 8.1. Comput Phys Commun 2008;178:852.
[27] Belyaev I, Brambach T, Brook NH, et al. Handling of the generation of primary events in Gauss, the LHCb simulation framework. J Phys Conf Ser 2011;331:032047.
[28] Lange DJ. The EvtGen particle decay simulation package. Nucl Instrum Meth 2001;A462:152.
[29] Davidson N, Przedzinski T, Was Z. PHOTOS interface in C++: technical and physics documentation. Comp Phys Comm 2016;199:86.
[30] Geant4 Collaboration, Allison J, et al. Geant4 developments and applications. IEEE Trans Nucl Sci 2006;53:270.
[31] Geant4 Collaboration, Agostinelli S, et al. Geant4: a simulation toolkit. Nucl Instrum Meth A 2003;506:250.
[32] Clemencic M, Corti G, Easo S, et al. The LHCb simulation application, Gauss: design, evolution and experience. J Phys Conf Ser 2011;331:032023.
[33] Müller D, Clemencic M, Corti G, et al. ReDecay: a novel approach to speed up the simulation at LHCb. Eur Phys J C 2018;78:1009.
[34] Breiman L, Friedman JH, Olshen RA, et al. Classification and regression trees. Belmont, California, USA: Wadsworth international group; 1984.
[35] Freund Y, Schapire RE. A decision-theoretic generalization of on-line learning and an application to boosting. J Comput Syst Sci 1997;55:119.
[36] Voss H, Hoecker A, Stelzer J, et al. TMVA – Toolkit for multivariate data analysis with ROOT. Proc Science (ACAT) 2007;040:1–12.
[37] Hoecker A, Speckmayer P, Stelzer J, et al. TMVA 4 — Toolkit for multivariate data analysis with ROOT, Users Guide. arXiv: 0703039, 2007.
[38] Particle Data Group, Zyla PA, et al. Review of particle physics. Prog Theor Exp Phys 2020;2020:083C01.
[39] Gulin A, Kuralenok I, Pavlov D. Winning the transfer learning track of Yahoo!'s learning to rank challenge with YetiRank. Proceedings of the 2010 International Conference on Yahoo! Learning to Rank 2010;14:63–76.
[40] LHCb Collaboration, Aaij R, et al. Performance of the LHCb trigger and full real-time reconstruction in Run 2 of the LHC. J Instrum 2019;14:P04013.
[41] Skwarnicki T. A study of the radiative cascade transitions between the Upsilon-prime and Upsilon resonances [Ph.D. thesis], Institute of Nuclear Physics, Krakow; 1986. DESY-F31-86-02.
[42] Bukin AD. Fitting function for asymmetric peaks. arXiv: 0711.4449, 2007.
[43] Pivk M, Le Diberder FR. sPlot: a statistical tool to unfold data distributions. Nucl Instrum Meth 2005;A555:356.
[44] Martin Sanchez A, Robbe P, Schune M-H. Performances of the LHCb L0 Calorimeter Trigger, LHCb-PUB-2011-026; CERN-LHCb-PUB-2011-026, CERN, Geneva; 2012.
[45] Hulsbergen WD. The global covariance matrix of tracks fitted with a Kalman filter and an application in detector alignment. Nucl Instrum Meth 2009; A600:471.
[46] Viret S, Parkes C, Gersabeck M. Alignment procedure of the LHCb vertex detector. Nucl Instrum Meth 2008;A596:157.

The LHCb experiment

LHCb is one of the four large experiments located on the Large Hadron Collider (LHC) at CERN. The LHCb detector is a single-arm forward spectrometer covering the pseudorapidity range $2 < \eta < 5$, designed for the study of particles containing *b* or *c* quarks. The detector includes a silicon-strip vertex detector surrounding the proton-proton interaction region, tracking stations on either side of a dipole magnet, ring-imaging Cherenkov (RICH) detectors, calorimeters and muon chambers. The LHCb Collaboration consists of more than 1400 members from 18 countries in 5 continents, including both physicists and engineers.

LHCb Collaboration

R. Aaij[32], A.S.W. Abdelmotteleb[56], C. Abellán Beteta[50], T. Ackernley[60], B. Adeva[46], M. Adinolfi[54], H. Afsharnia[9], C. Agapopoulou[13], C.A. Aidala[86], S. Aiola[25], Z. Ajaltouni[9], S. Akar[65], J. Albrecht[15], F. Alessio[48], M. Alexander[59], A. Alfonso Albero[45], Z. Aliouche[62], G. Alkhazov[38], P. Alvarez Cartelle[55], S. Amato[2], J.L. Amey[54], Y. Amhis[11], L. An[48], L. Anderlini[22], A. Andreianov[38], M. Andreotti[21], D. Ao[6], F. Archilli[17], A. Artamonov[44], M. Artuso[68], K. Arzymatov[42], E. Aslanides[10], M. Atzeni[50], B. Audurier[12], S. Bachmann[17], M. Bachmayer[49], J.J. Back[56], P. Baladron Rodriguez[46], V. Balagura[12], W. Baldini[21], J. Baptista Leite[1], M. Barbetti[22], R.J. Barlow[62], S. Barsuk[11], W. Barter[61], M. Bartolini[24], F. Baryshnikov[83], J.M. Basels[14], S. Bashir[34], G. Bassi[29], B. Batsukh[68], A. Battig[15], A. Bay[49], A. Beck[56], M. Becker[15], F. Bedeschi[29], I. Bediaga[1], A. Beiter[68], V. Belavin[42], S. Belin[27], V. Bellee[50], K. Belous[44], I. Belov[40], I. Belyaev[41], G. Bencivenni[23], E. Ben-Haim[13], A. Berezhnoy[40], R. Bernet[50], D. Berninghoff[17], H.C. Bernstein[68], C. Bertella[48], A. Bertolin[28], C. Betancourt[50], F. Betti[48], Ia. Bezshyiko[50], S. Bhasin[54], J. Bhom[35], L. Bian[73], M.S. Bieker[15], S. Bifani[53], P. Billoir[13], M. Birch[61], F.C.R. Bishop[55], A. Bitadze[62], A. Bizzeti[22,k], M. Bjørn[63], M.P. Blago[48], T. Blake[56], F. Blanc[49], S. Blusk[68], D. Bobulska[59], J.A. Boelhauve[15], O. Boente Garcia[46], T. Boettcher[65], A. Boldyrev[82], A. Bondar[43], N. Bondar[38,48], S. Borghi[62], M. Borisyak[42], M. Borsato[17], J.T. Borsuk[35], S.A. Bouchiba[49], T.J.V. Bowcock[60], A. Boyer[48], C. Bozzi[21], M.J. Bradley[61], S. Braun[66], A. Brea Rodriguez[46], M. Brodski[48], J. Brodzicka[35], A. Brossa Gonzalo[56], D. Brundu[27], A. Buonaura[50], L. Buonincontri[28], A.T. Burke[62], C. Burr[48], A. Bursche[72], A. Butkevich[39], J.S. Butter[32], J. Buytaert[48], W. Byczynski[48], S. Cadeddu[27], H. Cai[73], R. Calabrese[21,f], L. Calefice[15,13], L. Calero Diaz[23], S. Cali[23], R. Calladine[53], M. Calvi[26,j], M. Calvo Gomez[85], P. Camargo Magalhaes[54], P. Campana[23], A.F. Campoverde Quezada[6], S. Capelli[26,j], L. Capriotti[20,d], A. Carbone[20,d], G. Carboni[31], R. Cardinale[24], A. Cardini[27], I. Carli[4], P. Carniti[26,j], L. Carus[14], K. Carvalho Akiba[32], A. Casais Vidal[46], G. Casse[60], M. Cattaneo[48], G. Cavallero[48], S. Celani[49], J. Cerasoli[10], D. Cervenkov[63], A.J. Chadwick[60], M.G. Chapman[54], M. Charles[13], Ph. Charpentier[48], G. Chatzikonstantinidis[53], C.A. Chavez Barajas[60], M. Chefdeville[8], C. Chen[3], S. Chen[4], A. Chernov[35], V. Chobanova[46], S. Cholak[49], M. Chrzaszcz[35], A. Chubykin[38], V. Chulikov[38], P. Ciambrone[23], M.F. Cicala[56], X. Cid Vidal[46], G. Ciezarek[48], P.E.L. Clarke[58], M. Clemencic[48], H.V. Cliff[55], J. Closier[48], J.L. Cobbledick[62], V. Coco[48], J.A.B. Coelho[11], J. Cogan[10], E. Cogneras[9], L. Cojocariu[37], P. Collins[48], T. Colombo[48], L. Congedo[19,c], A. Contu[27], N. Cooke[53], G. Coombs[59], I. Corredoira Fernandez[46], G. Corti[48], C.M. Costa Sobral[56], B. Couturier[48], D.C. Craik[64], J. Crkovská[67], M. Cruz Torres[1], R. Currie[58], C.L. Da Silva[67], S. Dadabaev[83], L. Dai[71], E. Dall'Occo[15], J. Dalseno[46], C. D'Ambrosio[48], A. Danilina[41], P. d'Argent[48], J.E. Davies[62], A. Davis[62], O. De Aguiar Francisco[62], K. De Bruyn[79], S. De Capua[62], M. De Cian[49], J.M. De Miranda[1], L. De Paula[2], M. De Serio[19,c], D. De Simone[50], P. De Simone[23], J.A. de Vries[80], C.T. Dean[67], D. Decamp[8], V. Dedu[10], L. Del Buono[13], B. Delaney[55], H.-P. Dembinski[15], A. Dendek[34], V. Denysenko[50], D. Derkach[82],

O. Deschamps[9], F. Desse[11], F. Dettori[27,e], B. Dey[77], A. Di Cicco[23], P. Di Nezza[23], S. Didenko[83], L. Dieste Maronas[46], H. Dijkstra[48], V. Dobishuk[52], C. Dong[3], A.M. Donohoe[18], F. Dordei[27], A.C. dos Reis[1], L. Douglas[59], A. Dovbnya[51], A.G. Downes[8], M.W. Dudek[35], L. Dufour[48], V. Duk[78], P. Durante[48], J.M. Durham[67], D. Dutta[62], A. Dziurda[35], A. Dzyuba[38], S. Easo[57], U. Egede[69], V. Egorychev[41], S. Eidelman[43,v], S. Eisenhardt[58], S. Ek-In[49], L. Eklund[59,w], S. Ely[68], A. Ene[37], E. Epple[67], S. Escher[14], J. Eschle[50], S. Esen[13], T. Evans[48], A. Falabella[20], J. Fan[3], Y. Fan[6], B. Fang[73], S. Farry[60], D. Fazzini[26,j], M. Féo[48], A. Fernandez Prieto[46], J.M. Fernandez-tenllado Arribas[45], A.D. Fernez[66], F. Ferrari[20,d], L. Ferreira Lopes[49], F. Ferreira Rodrigues[2], S. Ferreres Sole[32], M. Ferrillo[50], M. Ferro-Luzzi[48], S. Filippov[39], R.A. Fini[19], M. Fiorini[21,f], M. Firlej[34], K.M. Fischer[63], D.S. Fitzgerald[86], C. Fitzpatrick[62], T. Fiutowski[34], A. Fkiaras[48], F. Fleuret[12], M. Fontana[13], F. Fontanelli[24,h], R. Forty[48], D. Foulds-Holt[55], V. Franco Lima[60], M. Franco Sevilla[66], M. Frank[48], E. Franzoso[21], G. Frau[17], C. Frei[48], D.A. Friday[59], J. Fu[25], Q. Fuehring[15], E. Gabriel[32], T. Gaintseva[42], A. Gallas Torreira[46], D. Galli[20,d], S. Gambetta[58,48], Y. Gan[3], M. Gandelman[2], P. Gandini[25], Y. Gao[5], M. Garau[27], L.M. Garcia Martin[56], P.GarciaMoreno[45], J. García Pardiñas[26,j], B. Garcia Plana[46], F.A. Garcia Rosales[12], L. Garrido[45], C. Gaspar[48], R.E. Geertsema[32], D. Gerick[17], L.L. Gerken[15], E. Gersabeck[62], M. Gersabeck[62], T. Gershon[56], D. Gerstel[10], Ph. Ghez[8], L. Giambastiani[28], V. Gibson[55], H.K. Giemza[36], A.L. Gilman[63], M. Giovannetti[23,p], A. Gioventù[46], P. Gironella Gironell[45], L. Giubega[37], C. Giugliano[21,f,48], K. Gizdov[58], E.L. Gkougkousis[48], V.V. Gligorov[13], C. Göbel[70], E. Golobardes[85], D. Golubkov[41], A. Golutvin[61,83], A. Gomes[1,a], S. Gomez Fernandez[45], F. Goncalves Abrantes[63], M. Goncerz[35], G. Gong[3], P. Gorbounov[41], I.V. Gorelov[40], C. Gotti[26], E. Govorkova[48], J.P. Grabowski[17], T. Grammatico[13], L.A. Granado Cardoso[48], E. Graugés[45], E. Graverini[49], G. Graziani[22], A. Grecu[37], L.M. Greeven[32], N.A. Grieser[4], L. Grillo[62], S. Gromov[83], B.R. Gruberg Cazon[63], C. Gu[3], M. Guarise[21], P. A. Günther[17], E. Gushchin[39], A. Guth[14], Y. Guz[44], T. Gys[48], T. Hadavizadeh[69], G. Haefeli[49], C. Haen[48], J. Haimberger[48], T. Halewood-leagas[60], P.M. Hamilton[66], J.P. Hammerich[60], Q. Han[7], X. Han[17], T.H. Hancock[63], S. Hansmann-Menzemer[17], N. Harnew[63], T. Harrison[60], C. Hasse[48], M. Hatch[48], J. He[6,b], M. Hecker[61], K. Heijhoff[32], K. Heinicke[15], A.M. Hennequin[48], K. Hennessy[60], L. Henry[48], J. Heuel[14], A. Hicheur[2], D. Hill[49], M. Hilton[62], S.E. Hollitt[15], J. Hu[17], J. Hu[72], W. Hu[7], X. Hu[3], W. Huang[6], X. Huang[73], W. Hulsbergen[32], R.J. Hunter[56], M. Hushchyn[82], D. Hutchcroft[60], D. Hynds[32], P. Ibis[15], M. Idzik[34], D. Ilin[38], P. Ilten[65], A. Inglessi[38], A. Ishteev[83], K. Ivshin[38], R. Jacobsson[48], S. Jakobsen[48], E. Jans[32], B.K. Jashal[47], A. Jawahery[66], V. Jevtic[15], M. Jezabek[35], F. Jiang[3], M. John[63], D. Johnson[48], C.R. Jones[55], T.P. Jones[56], B. Jost[48], N. Jurik[48], S.H. Kalavan Kadavath[34], S. Kandybei[51], Y. Kang[3], M. Karacson[48], M. Karpov[82], F. Keizer[48], M. Kenzie[56], T. Ketel[33], B. Khanji[15], A. Kharisova[84], S. Kholodenko[44], T. Kirn[14], V.S. Kirsebom[49], O. Kitouni[64], S. Klaver[32], N. Kleijne[29], K. Klimaszewski[36], M.R. Kmiec[36], S. Koliiev[52], A. Kondybayeva[83], A. Konoplyannikov[41], P. Kopciewicz[34], R. Kopecna[17], P. Koppenburg[32], M. Korolev[40], I. Kostiuk[32,52], O. Kot[52], S. Kotriakhova[21,38], P. Kravchenko[38], L. Kravchuk[39], R.D. Krawczyk[48], M. Kreps[56], F. Kress[61], S. Kretzschmar[14], P. Krokovny[43,v], W. Krupa[34], W. Krzemien[36], W. Kucewicz[35,t], M. Kucharczyk[35], V. Kudryavtsev[43,v], H.S. Kuindersma[32,33], G.J. Kunde[67], T. Kvaratskheliya[41], D. Lacarrere[48], G. Lafferty[62], A. Lai[27], A. Lampis[27], D. Lancierini[50], J.J. Lane[62], R. Lane[54], G. Lanfranchi[23], C. Langenbruch[14], J. Langer[15], O. Lantwin[83], T. Latham[56], F. Lazzari[29,q], R. Le Gac[10], S.H. Lee[86], R. Lefèvre[9], A. Leflat[40], S. Legotin[83], O. Leroy[10], T. Lesiak[35], B. Leverington[17], H. Li[72], P. Li[17], S. Li[7], Y. Li[4], Y. Li[4], Z. Li[68], X. Liang[68], T. Lin[61], R. Lindner[48], V. Lisovskyi[15], R. Litvinov[27], G. Liu[72], H. Liu[6], S. Liu[4], A. Lobo Salvia[45], A. Loi[27], J. Lomba Castro[46], I. Longstaff[59], J.H. Lopes[2], S. Lopez Solino[46], G.H. Lovell[55], Y. Lu[4], C. Lucarelli[22], D. Lucchesi[28,l], S. Luchuk[39], M. Lucio Martinez[32], V. Lukashenko[32], Y. Luo[3], A. Lupato[62], E. Luppi[21,f], O. Lupton[56], A. Lusiani[29,m], X. Lyu[6], L. Ma[4], R. Ma[6], S. Maccolini[20,d], F. Machefert[11], F. Maciuc[37], V. Macko[49], P. Mackowiak[15], S. Maddrell-Mander[54], O. Madejczyk[34], L.R. Madhan Mohan[54], O. Maev[38], A. Maevskiy[82], D. Maisuzenko[38], M.W. Majewski[34], J.J. Malczewski[35], S. Malde[63], B. Malecki[48], A. Malinin[81], T. Maltsev[43,v], H. Malygina[17], G. Manca[27,e], G. Mancinelli[10], D. Manuzzi[20,d], D. Marangotto[25,i], J. Maratas[9,s], J.F. Marchand[8], U. Marconi[20], S. Mariani[22,g], C. Marin Benito[48], M. Marinangeli[49], J. Marks[17], A.M. Marshall[54], P.J. Marshall[60], G. Martellotti[30], L. Martinazzoli[48,j], M. Martinelli[26,j], D. Martinez Santos[46], F. Martinez Vidal[47], A. Massafferri[1], M. Materok[14], R. Matev[48], A. Mathad[50], Z. Mathe[48], V. Matiunin[41], C. Matteuzzi[26], K.R. Mattioli[86], A. Mauri[32], E. Maurice[12], J. Mauricio[45], M. Mazurek[48], M. McCann[61], L. Mcconnell[18], T.H. Mcgrath[62], N.T. Mchugh[59], A. McNab[62], R. McNulty[18], J.V. Mead[60], B. Meadows[65], G. Meier[15], N. Meinert[76], D. Melnychuk[36], S. Meloni[26,j], M. Merk[32,80], A. Merli[25], L. Meyer Garcia[2], M. Mikhasenko[48], D.A. Milanes[74], E. Millard[56], M. Milovanovic[48], M.-N. Minard[8], A. Minotti[26,j], L. Minzoni[21,f], S.E. Mitchell[58], B. Mitreska[62], D.S. Mitzel[48], A. Mödden [15], R.A. Mohammed[63], R.D. Moise[61], T. Mombächer[46], I.A. Monroy[74], S. Monteil[9], M. Morandin[28], G. Morello[23], M.J. Morello[29,m], J. Moron[34], A.B. Morris[75], A.G. Morris[56], R. Mountain[68], H. Mu[3], F. Muheim[58,48], M. Mulder[48], D. Müller[48], K. Müller[50], C.H. Murphy[63], D. Murray[62], P. Muzzetto[27,48], P. Naik[54], T. Nakada[49], R. Nandakumar[57], T. Nanut[49], I. Nasteva[2],M.Needham[58], I. Neri[21], N. Neri[25,i], S. Neubert[75], N. Neufeld[48], R. Newcombe[61], T.D. Nguyen[49], C. Nguyen-Mau[49,x], E.M. Niel[11], S. Nieswand[14], N. Nikitin[40], N.S. Nolte[64], C. Normand[8], C. Nunez[86], A. Oblakowska-Mucha[34], V. Obraztsov[44], T. Oeser[14], D.P. O'Hanlon[54], S. Okamura[21], R. Oldeman[27,e], M.E. Olivares[68], C.J.G. Onderwater[79], R.H. O'neil[58], A. Ossowska[35], J.M. Otalora Goicochea[2], T. Ovsiannikova[41], P. Owen[50], A. Oyanguren[47], K.O. Padeken[75], B. Pagare[56], P.R. Pais[48], T. Pajero[63], A. Palano[19], M. Palutan[23], Y. Pan[62], G. Panshin[84], A. Papanestis[57], M. Pappagallo[19,c], L.L. Pappalardo[21,f], C. Pappenheimer[65], W. Parker[66], C. Parkes[62], B. Passalacqua[21], G. Passaleva[22], A. Pastore[19], M. Patel[61], C. Patrignani[20,d], C.J. Pawley[80], A. Pearce[48], A. Pellegrino[32], M. Pepe Altarelli[48], S. Perazzini[20], D. Pereima[41], A. Pereiro Castro[46], P. Perret[9], M. Petric[59,48], K. Petridis[54], A. Petrolini[24,h], A. Petrov[81], S. Petrucci[58], M. Petruzzo[25], T.T.H. Pham[68], A. Philippov[42], L. Pica[29,m], M. Piccini[78], B. Pietrzyk[8], G. Pietrzyk[49], M. Pili[63], D. Pinci[30], F. Pisani[48], M. Pizzichemi[48], Resmi P.K[10], V. Placinta[37], J. Plews[53], M. Plo Casasus[46], F. Polci[13], M. Poli Lener[23], M. Poliakova[68], A. Poluektov[10], N. Polukhina[83,u], I. Polyakov[68], E. Polycarpo[2], S. Ponce[48], D. Popov[6,48], S. Popov[42], S. Poslavskii[44], K. Prasanth[35], L. Promberger[48], C. Prouve[46], V. Pugatch[52], V. Puill[11], H. Pullen[63], G. Punzi[29,n], H. Qi[3], W. Qian[6], J. Qin[6], N. Qin[3], R. Quagliani[13], B. Quintana[8], N.V. Raab[18], R.I. Rabadan Trejo[6], B. Rachwal[34], J.H. Rademacker[54], M. Rama[29], M. Ramos Pernas[56], M.S. Rangel[2], F. Ratnikov[42,82], G. Raven[33], M. Reboud[8], F. Redi[49], F. Reiss[62], C. Remon Alepuz[47], Z. Ren[3], V. Renaudin[63], R. Ribatti[29], S. Ricciardi[57], K. Rinnert[60], P. Robbe[11], G. Robertson[58], A.B. Rodrigues[49], E. Rodrigues[60], J.A. Rodriguez Lopez[74], E. Rodriguez Rodriguez[46], A. Rollings[63], P. Roloff[48], V. Romanovskiy[44], M. Romero Lamas[46], A. Romero Vidal[46], J.D. Roth[86], M. Rotondo[23], M.S. Rudolph[68], T. Ruf[48], R.A. Ruiz Fernandez[46], J. Ruiz Vidal[47], A. Ryzhikov[82], J. Ryzka[34], J.J. Saborido Silva[46], N. Sagidova[38], N. Sahoo[56], B. Saitta[27,e], M. Salomoni[48], D. Sanchez Gonzalo[45], C. Sanchez Gras[32], R. Santacesaria[30], C. Santamarina Rios[46], M. Santimaria[23], E. Santovetti[31,p], D. Saranin[83], G. Sarpis[59], M. Sarpis[75], A. Sarti[30], C. Satriano[30,o], A. Satta[31], M. Saur[15], D. Savrina[41,40], H. Sazak[9], L.G. Scantlebury Smead[63], A. Scarabotto[13], S. Schael[14], S. Scherl[60], M. Schiller[59], H. Schindler[48], M. Schmelling[16], B. Schmidt[48], S. Schmitt[14],

O. Schneider[49], A. Schopper[48], M. Schubiger[32], S. Schulte[49], M.H. Schune[11], R. Schwemmer[48], B. Sciascia[23,48], S. Sellam[46], A. Semennikov[41], M. Senghi Soares[33], A. Sergi[24], N. Serra[50], L. Sestini[28], A. Seuthe[15], Y. Shang[5], D.M. Shangase[86], M. Shapkin[44], I. Shchemerov[83], L. Shchutska[49], T. Shears[60], L. Shekhtman[43,v], Z. Shen[5], V. Shevchenko[81], E.B. Shields[26,j], Y. Shimizu[11], E. Shmanin[83], J.D. Shupperd[68], B.G. Siddi[21], R. Silva Coutinho[50], G. Simi[28], S. Simone[19,c], N. Skidmore[62], T. Skwarnicki[68], M.W. Slater[53], I. Slazyk[21,f], J.C. Smallwood[63], J.G. Smeaton[55], A. Smetkina[41], E. Smith[14], M. Smith[61], A. Snoch[32], M. Soares[20], L. Soares Lavra[9], M.D. Sokoloff[65], F.J.P. Soler[59], A. Solovev[38], I. Solovyev[38], F.L. Souza De Almeida[2], B. Souza De Paula[2], B. Spaan[15], E. Spadaro Norella[25], P. Spradlin[59], F. Stagni[48], M. Stahl[65], S. Stahl[48], S. Stanislaus[63], O. Steinkamp[50,83], O. Stenyakin[44], H. Stevens[15], S. Stone[68], M.E. Stramaglia[49], M. Straticiuc[37], D. Strekalina[83], F. Suljik[63], J. Sun[27], L. Sun[73], Y. Sun[66], P. Svihra[62], P.N. Swallow[53], K. Swientek[34], A. Szabelski[36], T. Szumlak[34], M. Szymanski[48], S. Taneja[62], A.R. Tanner[54], M.D. Tat[63], A. Terentev[83], F. Teubert[48], E. Thomas[48], D.J.D. Thompson[53], K.A. Thomson[60], V. Tisserand[9], S. T'Jampens[8], M. Tobin[4], L. Tomassetti[21,f], X. Tong[5], D. Torres Machado[1], D.Y. Tou[13], M.T. Tran[49], E. Trifonova[83], C. Trippl[49], G. Tuci[29,n], A. Tully[49], N. Tuning[32,48], A. Ukleja[36], D.J. Unverzagt[17], E. Ursov[83], A. Usachov[32], A. Ustyuzhanin[42,82], U. Uwer[17], A. Vagner[84], V. Vagnoni[20], A. Valassi[48], G. Valenti[20], N. Valls Canudas[85], M. van Beuzekom[32], M. Van Dijk[49], E. van Herwijnen[83], C.B. Van Hulse[18], M. van Veghel[79], R. Vazquez Gomez[46], P. Vazquez Regueiro[46], C. Vázquez Sierra[48], S. Vecchi[21], J.J. Velthuis[54], M. Veltri[22,r], A. Venkateswaran[68], M. Veronesi[32], M. Vesterinen[56], D. Vieira[65], M. Vieites Diaz[49], H. Viemann[76], X. Vilasis-Cardona[85], E. Vilella Figueras[60], A. Villa[20], P. Vincent[13], F.C. Volle[11], D. Vom Bruch[10], A. Vorobyev[38], V. Vorobyev[43,v], N. Voropaev[38], K. Vos[80], R. Waldi[17], J. Walsh[29], C. Wang[17], J. Wang[5], J. Wang[4], J. Wang[3], J. Wang[73], M. Wang[3], R. Wang[54], Y. Wang[7], Z. Wang[50], Z. Wang[3], J.A. Ward[56], H.M. Wark[60],N.K.Watson[53], S.G. Weber[13], D. Websdale[61], C. Weisser[64], B.D.C. Westhenry[54], D.J. White[62], M. Whitehead[54], A.R. Wiederhold[56], D. Wiedner[15], G. Wilkinson[63], M. Wilkinson[68], I. Williams[55], M. Williams[64], M.R.J. Williams[58], F.F. Wilson[57], W. Wislicki[36], M. Witek[35], L. Witola[17], G. Wormser[11], S.A. Wotton[55], H. Wu[68], K. Wyllie[48], Z. Xiang[6], D. Xiao[7], Y. Xie[7], A. Xu[5], J. Xu[6], L. Xu[3], M. Xu[7], Q. Xu[6], Z. Xu[5], Z. Xu[6], D. Yang[3], S. Yang[6], Y. Yang[6], Z. Yang[5], Z. Yang[66], Y. Yao[68], L.E. Yeomans[60], H. Yin[7], J. Yu[71], X. Yuan[68], O. Yushchenko[44], E. Zaffaroni[49], M. Zavertyaev[16,u], M. Zdybal[35], O. Zenaiev[48], M. Zeng[3], D. Zhang[7], L. Zhang[3], S. Zhang[71], S. Zhang[5], Y. Zhang[5], Y. Zhang[63], A. Zharkova[83], A. Zhelezov[17], Y. Zheng[6], T. Zhou[5], X. Zhou[6], Y. Zhou[6], V. Zhovkovska[11], X. Zhu[3], Z. Zhu[6], V. Zhukov[14,40], J.B. Zonneveld[58], Q. Zou[4], S. Zucchelli[20,d], D. Zuliani[28], G. Zunica[62].

[1] Centro Brasileiro de Pesquisas Físicas (CBPF), Rio de Janeiro, Brazil
[2] Universidade Federal do Rio de Janeiro (UFRJ), Rio de Janeiro, Brazil
[3] Center for High Energy Physics, Tsinghua University, Beijing, China
[4] Institute Of High Energy Physics (IHEP), Beijing, China
[5] School of Physics State Key Laboratory of Nuclear Physics and Technology, Peking University, Beijing, China
[6] University of Chinese Academy of Sciences, Beijing, China
[7] Institute of Particle Physics, Central China Normal University, Wuhan, Hubei, China
[8] Univ. Savoie Mont Blanc, CNRS, IN2P3-LAPP, Annecy, France
[9] Université Clermont Auvergne, CNRS/IN2P3, LPC, Clermont-Ferrand, France
[10] Aix Marseille Univ, CNRS/IN2P3, CPPM, Marseille, France
[11] Université Paris-Saclay, CNRS/IN2P3, IJCLab, Orsay, France
[12] Laboratoire Leprince-Ringuet, CNRS/IN2P3, Ecole Polytechnique, Institut Polytechnique de Paris, Palaiseau, France
[13] LPNHE, Sorbonne Université, Paris Diderot Sorbonne Paris Cité, CNRS/IN2P3, Paris, France
[14] I. Physikalisches Institut, RWTH Aachen University, Aachen, Germany
[15] Fakultät Physik, Technische Universität Dortmund, Dortmund, Germany
[16] Max-Planck-Institut für Kernphysik (MPIK), Heidelberg, Germany
[17] Physikalisches Institut, Ruprecht-Karls-Universität Heidelberg, Heidelberg, Germany
[18] School of Physics, University College Dublin, Dublin, Ireland
[19] INFN Sezione di Bari, Bari, Italy
[20] INFN Sezione di Bologna, Bologna, Italy
[21] INFN Sezione di Ferrara, Ferrara, Italy
[22] INFN Sezione di Firenze, Firenze, Italy
[23] INFN Laboratori Nazionali di Frascati, Frascati, Italy
[24] INFN Sezione di Genova, Genova, Italy
[25] INFN Sezione di Milano, Milano, Italy
[26] INFN Sezione di Milano-Bicocca, Milano, Italy
[27] INFN Sezione di Cagliari, Monserrato, Italy
[28] Universita degli Studi di Padova, Universita e INFN, Padova, Padova, Italy
[29] INFN Sezione di Pisa, Pisa, Italy
[30] INFN Sezione di Roma La Sapienza, Roma, Italy
[31] INFN Sezione di Roma Tor Vergata, Roma, Italy
[32] Nikhef National Institute for Subatomic Physics, Amsterdam, Netherlands
[33] Nikhef National Institute for Subatomic Physics and VU University Amsterdam, Amsterdam, Netherlands
[34] AGH - University of Science and Technology, Faculty of Physics and Applied Computer Science, Kraków, Poland
[35] Henryk Niewodniczanski Institute of Nuclear Physics Polish Academy of Sciences, Kraków, Poland
[36] National Center for Nuclear Research (NCBJ), Warsaw, Poland
[37] Horia Hulubei National Institute of Physics and Nuclear Engineering, Bucharest-Magurele, Romania
[38] Petersburg Nuclear Physics Institute NRC Kurchatov Institute (PNPI NRC KI), Gatchina, Russia
[39] Institute for Nuclear Research of the Russian Academy of Sciences (INR RAS), Moscow, Russia
[40] Institute of Nuclear Physics, Moscow State University (SINP MSU), Moscow, Russia
[41] Institute of Theoretical and Experimental Physics NRC Kurchatov Institute (ITEP NRC KI), Moscow, Russia
[42] Yandex School of Data Analysis, Moscow, Russia
[43] Budker Institute of Nuclear Physics (SB RAS), Novosibirsk, Russia
[44] Institute for High Energy Physics NRC Kurchatov Institute (IHEP NRC KI), Protvino, Russia, Protvino, Russia
[45] ICCUB, Universitat de Barcelona, Barcelona, Spain
[46] Instituto Galego de Física de Altas Enerxías (IGFAE), Universidade de Santiago de Compostela, Santiago de Compostela, Spain
[47] Instituto de Fisica Corpuscular, Centro Mixto Universidad de Valencia - CSIC, Valencia, Spain
[48] European Organization for Nuclear Research (CERN), Geneva, Switzerland
[49] Institute of Physics, Ecole Polytechnique Fédérale de Lausanne (EPFL), Lausanne, Switzerland
[50] Physik-Institut, Universität Zürich, Zürich, Switzerland
[51] NSC Kharkiv Institute of Physics and Technology (NSC KIPT), Kharkiv, Ukraine
[52] Institute for Nuclear Research of the National Academy of Sciences (KINR), Kyiv, Ukraine
[53] University of Birmingham, Birmingham, United Kingdom

[54] H.H. Wills Physics Laboratory, University of Bristol, Bristol, United Kingdom
[55] Cavendish Laboratory, University of Cambridge, Cambridge, United Kingdom
[56] Department of Physics, University of Warwick, Coventry, United Kingdom
[57] STFC Rutherford Appleton Laboratory, Didcot, United Kingdom
[58] School of Physics and Astronomy, University of Edinburgh, Edinburgh, United Kingdom
[59] School of Physics and Astronomy, University of Glasgow, Glasgow, United Kingdom
[60] Oliver Lodge Laboratory, University of Liverpool, Liverpool, United Kingdom
[61] Imperial College London, London, United Kingdom
[62] Department of Physics and Astronomy, University of Manchester, Manchester, United Kingdom
[63] Department of Physics, University of Oxford, Oxford, United Kingdom
[64] Massachusetts Institute of Technology, Cambridge, MA, United States
[65] University of Cincinnati, Cincinnati, OH, United States
[66] University of Maryland, College Park, MD, United States
[67] Los Alamos National Laboratory (LANL), Los Alamos, United States
[68] Syracuse University, Syracuse, NY, United States
[69] School of Physics and Astronomy, Monash University, Melbourne, Australia, associated to [56]
[70] Pontifícia Universidade Católica do Rio de Janeiro (PUC-Rio), Rio de Janeiro, Brazil, associated to [2]
[71] Physics and Micro Electronic College, Hunan University, Changsha City, China, associated to [7]
[72] Guangdong Provencial Key Laboratory of Nuclear Science, Institute of Quantum Matter, South China Normal University, Guangzhou, China, associated to [3]
[73] School of Physics and Technology, Wuhan University, Wuhan, China, associated to [3]
[74] Departamento de Fisica , Universidad Nacional de Colombia, Bogota, Colombia, associated to [13]
[75] Universität Bonn - Helmholtz-Institut für Strahlen und Kernphysik, Bonn, Germany, associated to [17]
[76] Institut für Physik, Universität Rostock, Rostock, Germany, associated to [17]
[77] Eotvos Lorand University, Budapest, Hungary, associated to [48]
[78] INFN Sezione di Perugia, Perugia, Italy, associated to [21]
[79] Van Swinderen Institute, University of Groningen, Groningen, Netherlands, associated to [32]
[80] Universiteit Maastricht, Maastricht, Netherlands, associated to [32]
[81] National Research Centre Kurchatov Institute, Moscow, Russia, associated to [41]
[82] National Research University Higher School of Economics, Moscow, Russia, associated to [42]
[83] National University of Science and Technology "MISIS", Moscow, Russia, associated to [41]
[84] National Research Tomsk Polytechnic University, Tomsk, Russia, associated to [41]
[85] DS4DS, La Salle, Universitat Ramon Llull, Barcelona, Spain, associated to [45]
[86] University of Michigan, Ann Arbor, United States, associated to [68]
[a] Universidade Federal do Triângulo Mineiro (UFTM), Uberaba-MG, Brazil
[b] Hangzhou Institute for Advanced Study, UCAS, Hangzhou, China
[c] Università di Bari, Bari, Italy
[d] Università di Bologna, Bologna, Italy
[e] Università di Cagliari, Cagliari, Italy
[f] Università di Ferrara, Ferrara, Italy
[g] Università di Firenze, Firenze, Italy
[h] Università di Genova, Genova, Italy
[i] Università degli Studi di Milano, Milano, Italy
[j] Università di Milano Bicocca, Milano, Italy
[k] Università di Modena e Reggio Emilia, Modena, Italy
[l] Università di Padova, Padova, Italy
[m] Scuola Normale Superiore, Pisa, Italy
[n] Università di Pisa, Pisa, Italy
[o] Università della Basilicata, Potenza, Italy
[p] Università di Roma Tor Vergata, Roma, Italy
[q] Università di Siena, Siena, Italy
[r] Università di Urbino, Urbino, Italy
[s] MSU - Iligan Institute of Technology (MSU-IIT), Iligan, Philippines
[t] AGH - University of Science and Technology, Faculty of Computer Science, Electronics and Telecommunications, Kraków, Poland
[u] P.N. Lebedev Physical Institute, Russian Academy of Science (LPI RAS), Moscow, Russia
[v] Novosibirsk State University, Novosibirsk, Russia
[w] Department of Physics and Astronomy, Uppsala University, Uppsala, Sweden
[x] Hanoi University of Science, Hanoi, Vietnam